M., Hayashizaki, Y., and Puca, G. A. (1997) *Hum. Mol. Genet.* 6, 601–607
27. Iwata, Y., Katanosaka, Y., Arai, Y., Komamura, K., Miyatake, K., and Shigekawa, M. (2003) *J. Cell Biol.* 161, 957–967
28. Taigen, T., De Windt, L. J., Lim, H. W., and Molkentin, J. D. (2000) *Proc. Natl. Acad. Sci. U. S. A.* 97, 1196–1201
29. De Windt, L. J., Lim, H. W., Haq, S., Force, T., and Molkentin, J. D. (2000) *J. Biol. Chem.* 275, 13571–13579
30. Bueno, O. F., Wilkins, B. J., Tymitz, K. M., Glascock, B. J., Kimball, T. F., Lorenz, J. N., and Molkentin, J. D. (2002) *Proc. Natl. Acad. Sci. U. S. A.* 99, 4586–4991
31. Schwarz, E. M., and Benzer, S. (1997) *Proc. Natl. Acad. Sci. U. S. A.* 94, 10249–10254
32. Braz, J. C., Bueno, O. F., De Windt, L. J., and Molkentin, J. D. (2002) *J. Cell Biol.* 156, 905–919
33. Wang, Z., Nolan, B., Kutschke, W., and Hill, J. A. (2001) *J. Biol. Chem.* 276, 17706–17711

Acta Physiol Scand 2005, 184, 187–193

Myocardial interstitial choline and glutamate levels during acute myocardial ischaemia and local ouabain administration

T. Kawada,[1] T. Yamazaki,[2] T. Akiyama,[2] T. Shishido,[1] H. Mori[2] and M. Sugimachi[1]

1 *Department of Cardiovascular Dynamics, National Cardiovascular Center Research Institute, Osaka, Japan*

2 *Department of Cardiac Physiology, National Cardiovascular Center Research Institute, Osaka, Japan*

Received 25 November 2004, accepted 16 March 2005
Correspondence: T. Kawada, Department of Cardiovascular Dynamics, National Cardiovascular Center Research Institute, 5-7-1 Fujishirodai, Suita, Osaka 565-8565, Japan.
E-mail: torukawa@res.ncvc.go.jp

Abstract

Aim: Noradrenaline (NA) uptake transporters are known to reverse their action during acute myocardial ischaemia and to contribute to ischaemia-induced myocardial interstitial NA release. By contrast, functional roles of choline and glutamate transporters during acute myocardial ischaemia remain to be investigated. Because both transporters are driven by the normal Na^+ gradient across the plasma membrane in a similar manner to NA transporters, the loss of Na^+ gradient would affect the transporter function, which would in turn alter myocardial interstitial choline and glutamate levels. The aim of the present study was to examine the effects of acute myocardial ischaemia and the inhibition of Na^+,K^+-ATPase on myocardial interstitial glutamate and choline levels.

Methods: In anaesthetized cats, we measured myocardial interstitial glutamate and choline levels while inducing acute myocardial ischaemia or inhibiting Na^+,K^+-ATPase by local administration of ouabain.

Results: The choline level was not changed significantly by ischaemia (from 0.93 ± 0.06 to 0.82 ± 0.13 μM, mean ± SE, $n = 6$) and was decreased slightly by ouabain (from 1.30 ± 0.06 to 1.05 ± 0.07 μM, $P < 0.05$, $n = 6$). The glutamate level was significantly increased from 9.5 ± 1.9 to 34.7 ± 6.1 μM by ischaemia ($P < 0.01$, $n = 6$) and from 8.9 ± 1.0 to 15.9 ± 2.3 μM by ouabain ($P < 0.05$, $n = 6$). Inhibition of glutamate transport by *trans*-L-pyrrolidine-2,4-dicarboxylate (*t*-PDC) suppressed ischaemia- and ouabain-induced glutamate release.

Conclusion: Myocardial interstitial choline level was not increased by acute myocardial ischaemia or by Na^+,K^+-ATPase inhibition. By contrast, myocardial interstitial glutamate level was increased by both interventions. The glutamate transporter contributed to glutamate release via retrograde transport.

Keywords acetylcholine, cardiac microdialysis, cats, coronary artery occlusion, myocardium, noradrenaline.

Acute myocardial ischaemia causes oxygen depletion and loss of ATP in the ischaemic region (Hearse 1979). Blockade of H^+-ATPase leads to noradrenaline (NA) leakage from storage vesicles and axoplasmic NA accumulation (Schömig *et al.* 1988). Intracellular acidosis causes Na^+ influx via Na^+/H^+ exchange. Inhibition of Na^+,K^+-ATPase activity reduces the Na^+ gradient across the plasma membrane. Because NA uptake transporters are driven by the normal Na^+ electrochemical gradient across the plasma membrane,

© 2005 Scandinavian Physiological Society

axoplasmic NA accumulation and reduction of the Na^+ gradient cause reverse transport of NA from the intracellular space to the extracellular space (Schwartz 2000). Acute myocardial ischaemia evokes the myocardial interstitial NA release in the ischaemic region via retrograde NA transport, independently of efferent sympathetic nerve activity (Schömig *et al.* 1984, Yamazaki *et al.* 1996, Akiyama & Yamazaki 1999, Kawada *et al.* 2001a).

Similar to NA, choline and glutamate are taken up into cells by plasma membrane transporters driven by the Na^+ gradient (Schwartz 2000). We hypothesized that the loss of Na^+ gradient under ischaemic conditions would interfere with the transporter function, which would in turn alter myocardial interstitial choline and glutamate levels. Choline release has been suggested as an index of ischaemic degradation of the myocardial phospholipid bilayer in isolated, Tyrode solution-perfused rat hearts (Brühl *et al.* 2004). Glutamate can be a preferred myocardial fuel during ischaemia and may have protective effects on ischaemic myocardium (Arsenian 1998). Measuring myocardial interstitial levels of these molecules *in vivo* would contribute to understanding the pathophysiology of acute myocardial ischaemia. To test the hypothesis, we employed an *in vivo* cardiac microdialysis technique and measured myocardial interstitial choline and glutamate levels in anaesthetized cats (Akiyama *et al.* 1991, 1994, Yamazaki *et al.* 1997, Kawada *et al.* 2001b). Acute myocardial ischaemia inevitably affects systemic haemodynamics and perfusion of the heart. To minimize such haemodynamic effects, we also examined the effects of Na^+,K^+-ATPase inhibition on the myocardial interstitial choline and glutamate levels by locally administering ouabain through a dialysis probe (Yamazaki *et al.* 1999, Kawada *et al.* 2002). The results of the present study indicated that the myocardial interstitial choline level was not increased by acute myocardial ischaemia or by Na^+,K^+-ATPase inhibition. By contrast, the myocardial interstitial glutamate level was increased by both interventions. The glutamate transporter contributed to glutamate release via retrograde transport.

Materials and methods

Surgical preparation

Animal care was conducted in strict accordance with the *Guiding Principles for the Care and Use of Animals in the Field of Physiological Sciences* approved by the Physiological Society of Japan. Adult cats weighing 2.0–4.8 kg were anaesthetized via an intraperitoneal injection of pentobarbital sodium (30–35 mg kg^{-1}) and ventilated mechanically with room air mixed with oxygen. The depth of anaesthesia was maintained with a continuous intravenous infusion of pentobarbital sodium (1–2 mg kg^{-1} h^{-1}) through a catheter inserted via the right femoral vein. Mean systemic arterial pressure was monitored from a catheter inserted via the right femoral artery.

With the animal in the lateral position, the left fifth and sixth ribs were resected to expose the heart. When a coronary occlusion was necessary, a 3-0 silk suture was prepared around the left anterior descending coronary artery (LAD) just distal to the first diagonal branch. With a fine guiding needle, a dialysis probe was implanted into the left ventricular free wall perfused by the LAD. Heparin sodium (100 U kg^{-1} bolus injection followed by a maintenance dose of 50 U kg^{-1} h^{-1}) was administered intravenously to prevent blood coagulation. At the end of the experiment the experimental animals were killed by an overdose of pentobarbital sodium. We confirmed that the dialysis probe had been implanted within the left ventricular myocardium.

Dialysis technique

We designed a transverse dialysis probe (Akiyama *et al.* 1991, 1994). For measurements of small molecular compounds including ACh, choline, and glutamate, we used a dialysis fibre of 50 000 molecular weight cutoff (13 mm length, 310 μm OD, 200 μm ID; PAN-1200, Asahi Chemical, Osaka, Japan) with both ends glued to polyethylene tubes (20 cm length, 500 μm OD, 200 μm ID). The dialysis probe was perfused at a rate of 2 μL min^{-1} with Ringer solution. Each sample was collected in a microtube containing 3 μL of phosphate buffer (100 mM, pH 3.5). A cholinesterase inhibitor eserine (100 μM) was added to the perfusate to measure ACh. A preliminary examination indicated that whether the perfusate-contained eserine did not affect myocardial interstitial choline levels significantly. Dead space volume between the dialysis fibre and the sample microtube was identical for ACh, choline, and glutamate measurements, and the sampling was performed taking into account the time for dialysate to traverse the dead space volume.

The dialysate ACh and choline levels were measured directly by high-performance liquid chromatography with electrochemical detection. The absolute detection limits of ACh and choline, determined with a signal-to-noise ratio of 3, were 10 and 5 fmol per injection, respectively. The dialysate glutamate level was measured by kinetic enzymatic analysis with CMA 600. The absolute detection limit of glutamate was 1 μM per injection.

Protocols

All protocols were started from 2 h after implanting the dialysis probe. To examine changes in myocardial

© 2005 Scandinavian Physiological Society

interstitial ACh and choline levels during acute myocardial ischaemia ($n = 6$), after collecting a 15-min baseline dialysate sample, we occluded the LAD for 60 min and obtained four consecutive 15-min dialysate samples. The full-length of the implanted dialysis fibre was located within the ischaemic area judged by discolouration of myocardium during the LAD occlusion. We then released the occlusion and collected a 15-min dialysate sample during reperfusion. To examine changes in myocardial ACh and choline levels in response to local ouabain administration ($n = 6$), after collecting a 15-min baseline dialysate sample, we replaced the perfusate with Ringer solution containing 100 μM ouabain and collected four consecutive 15-min dialysate samples.

In different groups of animals, myocardial interstitial glutamate levels were measured during acute myocardial ischaemia ($n = 6$) and during local administration of ouabain ($n = 6$). To elucidate the role of the glutamate transporter, we also examined the effects of glutamate transport inhibition by *trans*-L-pyrrolidine-2,4-dicarboxylate (*t*-PDC, 10 mM) on myocardial interstitial glutamate levels during acute myocardial ischaemia ($n = 7$) and local administration of ouabain ($n = 7$). *t*-PDC was locally administered through the dialysis probe to avoid systemic effects.

Statistical analysis

All data are presented as mean ± SE values. In each protocol, the effects of myocardial ischaemia or local ouabain administration were examined using one-way analysis of variance followed by Dunnett's test against the corresponding baseline level (Glantz 2002). The baseline as well as maximum glutamate levels with and without glutamate transport inhibition were compared by an unpaired *t*-test during acute myocardial ischaemia or during local ouabain administration (Glantz 2002). Differences were considered to be significant when $P < 0.05$.

Results

Figure 1a shows myocardial interstitial ACh level during acute myocardial ischaemia. The ACh level was increased by LAD occlusion, becoming approximately 15 times higher than the baseline level at 30–45 and 45–60 min of ischaemia. The ACh level decreased towards the baseline level upon reperfusion. Figure 1b illustrates myocardial interstitial choline level during acute myocardial ischaemia. The choline level did not change significantly throughout the ischaemic and reperfusion periods.

Figure 2a shows changes in myocardial interstitial ACh level during local administration of ouabain. The ACh level was increased by the inhibition of

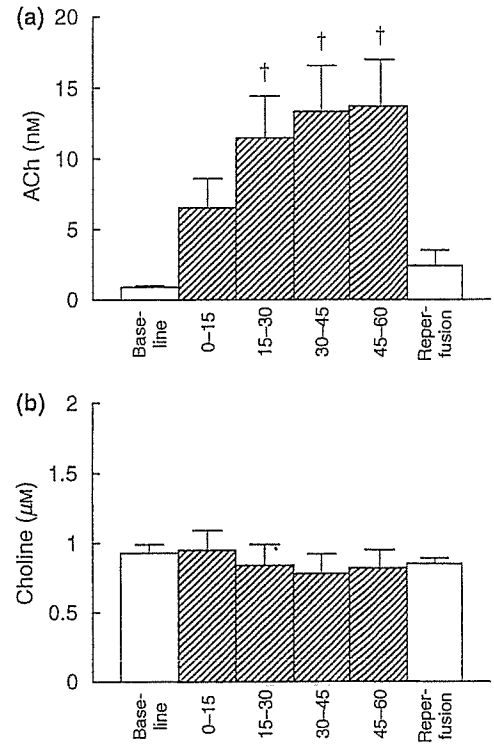

Figure 1 Changes in myocardial interstitial acetylcholine (ACh) level (a) and choline level (b) during coronary artery occlusion and reperfusion. Myocardial interstitial ACh level was significantly increased by acute myocardial ischaemia, while myocardial interstitial choline level was not changed. Data are mean ± SE. †$P < 0.01$ from baseline.

Na^+,K^+-ATPase, becoming approximately nine times higher than the baseline level at 15–30 min. The ACh level then decreased but remained significantly higher than the baseline level. Figure 2b illustrates the myocardial interstitial choline level during local administration of ouabain. The choline level was significantly lower at 0–15 and 45–60 min when compared with the baseline level.

Figure 3a shows changes in myocardial interstitial glutamate level during acute myocardial ischaemia. LAD occlusion increased the glutamate level to approximately 3.5 times higher than the baseline level at 0–15 min. Thereafter, the glutamate level was significantly higher than the baseline level throughout the ischaemic and reperfusion periods. Figure 3b illustrates the effects of glutamate transport inhibition on the ischaemia-induced glutamate release. The baseline glutamate level was significantly decreased by glutamate transport inhibition ($P < 0.05$). Although acute myocardial ischaemia and reperfusion significantly increased the glutamate level relative to the baseline level, the maximum glutamate level was attenuated to approximately one-fifth compared with that observed without glutamate transport inhibition ($P < 0.05$).

© 2005 Scandinavian Physiological Society

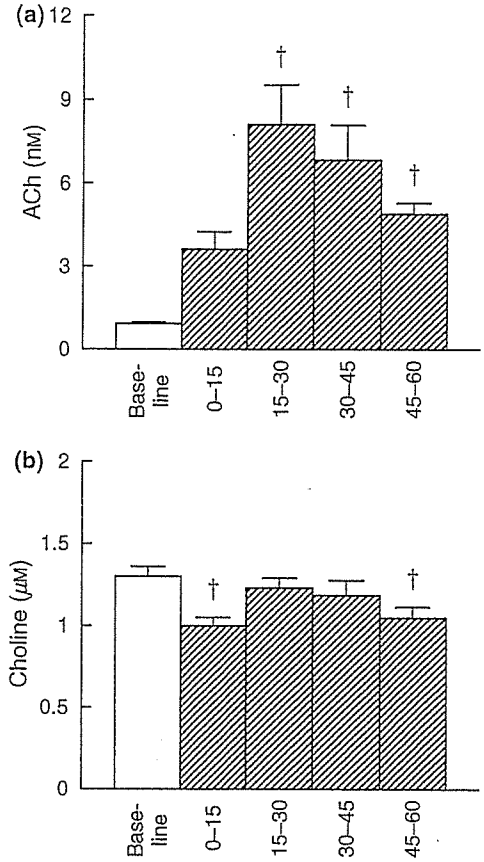

Figure 2 Changes in myocardial interstitial acetylcholine (ACh) level (a) and choline level (b) in response to the local administration of ouabain. Myocardial interstitial ACh level was significantly increased by ouabain. In contrast, myocardial interstitial choline level was decreased by ouabain. Data are mean ± SE. †$P < 0.01$ from baseline.

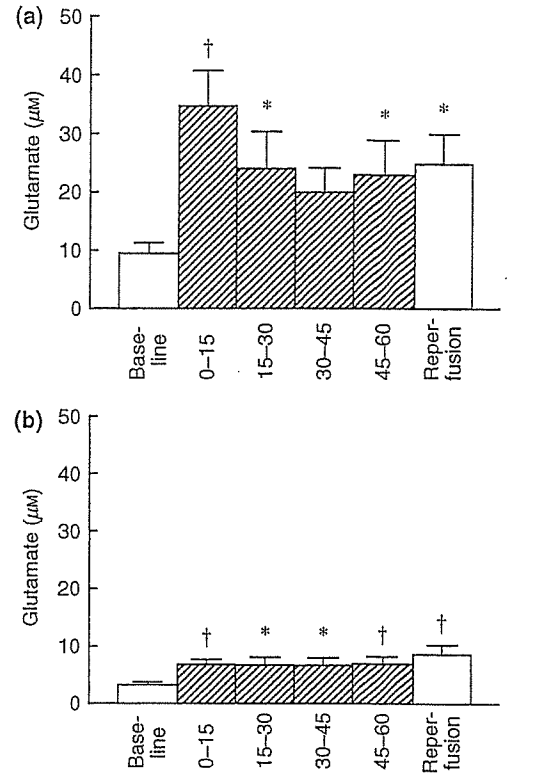

Figure 3 Changes in myocardial interstitial glutamate level during coronary artery occlusion and reperfusion without (a) and with (b) the inhibition of glutamate transporter. The glutamate level was significantly increased by acute myocardial ischaemia. The ischaemia-induced glutamate release was suppressed by the inhibition of glutamate transporter. Data are mean ± SE. †$P < 0.01$ and *$P < 0.05$ from baseline.

Figure 4a shows changes in myocardial interstitial glutamate level during the local administration of ouabain. Ouabain administration did not change the glutamate level at 0–15 min but increased the glutamate level thereafter. The glutamate level became approximately 1.8 times higher than the baseline level at 30–45 min. Figure 4b illustrates the effects of glutamate transport inhibition on ouabain-induced glutamate release. The baseline glutamate level was significantly decreased by the inhibition of glutamate transport ($P < 0.05$). Although ouabain administration increased the glutamate level relative to the baseline level, the maximum glutamate level was suppressed to approximately one-third of that observed without glutamate transport inhibition ($P < 0.05$).

Discussion

We have shown that acute myocardial ischaemia and local inhibition of Na^+,K^+-ATPase increased myocardial interstitial glutamate level but not choline level. Despite the similar Na^+ gradient dependency of corresponding transporters, myocardial interstitial glutamate and choline levels showed differential responses to the two interventions.

Changes in myocardial interstitial choline level

In the vagal nerve endings, ACh is hydrolysed to acetate and choline by acetylcholinesterase (Nicholls 1994). Choline is then taken up into the vagal nerve endings by the choline transporter driven by the Na^+ gradient. We hypothesized that loss of Na^+ gradient during acute myocardial ischaemia or local ouabain administration would increase the myocardial interstitial choline level by the interruption of choline uptake. Contrary to our hypothesis, acute myocardial ischaemia did not change myocardial interstitial choline level in the ischaemic region (Fig. 1b). Ouabain administration decreased the myocardial interstitial choline level at 0–15 and 45–60 min (Fig. 2b).

© 2005 Scandinavian Physiological Society

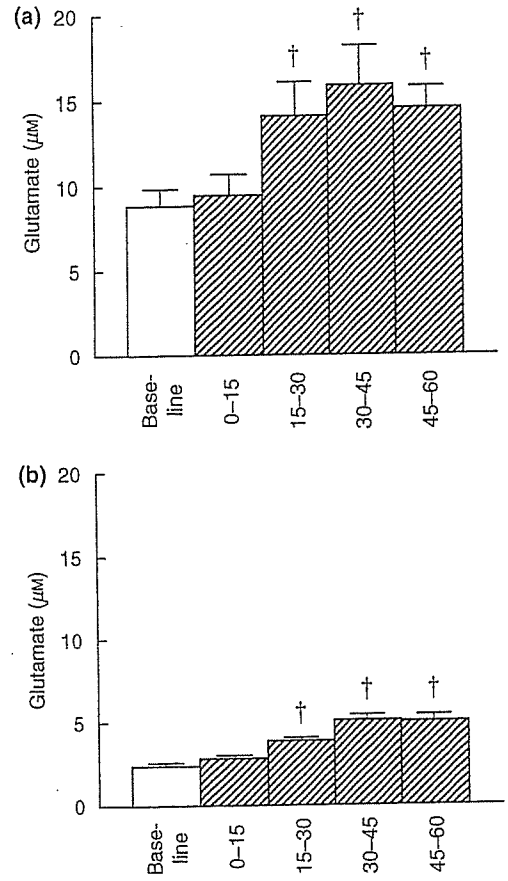

Figure 4 Changes in myocardial interstitial glutamate level in response to the local administration of ouabain without (a) and with (b) the inhibition of glutamate transporter. The glutamate level was significantly increased by ouabain administration. The ouabain-induced glutamate release was suppressed by the inhibition of glutamate transporter. Data are mean ± SE. †$P < 0.01$ from baseline.

Possible explanations for the absence of ischaemia- or ouabain-induced choline release are as follows. First, choline uptake is the rate-limiting step for ACh synthesis (Lockman & Allen 2002). Because choline in the intracellular space is rapidly consumed for ACh synthesis, the axoplasmic choline concentration might have been too low to evoke reverse transport by the choline transporter. Second, plasma choline concentration is stabilized by *de novo* choline synthesis from the catabolism of phosphatidylcholine found in cell membranes (Lockman & Allen 2002). Potential choline release may have been counterbalanced by the local stabilization mechanisms. Taking into account the recovery rate of the dialysis probe (approximately 30%), the myocardial interstitial choline concentration was 3–5 μM. Although the estimated concentration was lower than the highly regulated plasma choline concentration of approximately 10 μM, it was much higher than the ischaemia-induced maximum choline release (approximately 0.6 μM) in isolated rat hearts reported by Brühl *et al.* (2004). The present results suggest that myocardial interstitial choline level may not serve as an indicator of myocardial ischaemia in blood-perfused *in vivo* feline hearts.

By contrast with myocardial interstitial choline level, myocardial interstitial ACh level was increased both by acute myocardial ischaemia and by local administration of ouabain. Because ischaemia-induced ACh release was observed after vagal nerve transection in a previous study (Kawada *et al.* 2000), a Ca^{2+} channel-independent, regional release mechanism appears to be involved. Several reports have suggested that ouabain or ischaemia-induced intracellular Na^+ accumulation could elevate intracellular Ca^{2+} level via Na^+/Ca^{2+} exchange (Mochizuki & Jiang 1998, Li *et al.* 2000). The elevation of intracellular Ca^{2+} level may be associated with ACh release. Our previous study indicated that intracellular Ca^{2+} overload due to Ca^{2+} mobilization is responsible for the ACh release evoked by ischaemia (Kawada *et al.* 2000).

Changes in myocardial interstitial glutamate levels

Although the glutamate transporter family differs from the NA transporter family in that it requires counter-transport of K^+ instead of cotransport of Cl^-, its primary driving force is the Na^+ gradient across the plasma membrane (Schwartz 2000). Therefore, interventions that reduce the Na^+ gradient are likely to cause reverse transport of glutamate, in a similar manner to the reverse transport of NA. Acute myocardial ischaemia increased the myocardial interstitial glutamate level (Fig. 3a) as consistent with previous reports (Kennergren *et al.* 1997, 1999, Bäckström *et al.* 2003, Song *et al.* 1996). Inhibition of Na^+,K^+-ATPase also induced myocardial interstitial glutamate release (Fig. 4a). Glutamate release during acute myocardial ischaemia and local ouabain administration was significantly attenuated by the inhibition of glutamate transport (Figs 3b and 4b), suggesting the involvement of reverse transport by the glutamate transporter. Glutamate plays a vital role in keeping nitrogen balance in cells as a common amino acid in transamination reactions. The high intra-to-extracellular concentration ratio of glutamate would contribute to the retrograde transport by the glutamate transporter during the loss of normal Na^+ gradient.

In the case of myocardial interstitial NA levels, local blockade of NA uptake increased baseline NA levels, suggesting the accumulation of NA spontaneously released into the synaptic cleft (Akiyama & Yamazaki 1999). We therefore predicted that the inhibition of glutamate transport would increase the baseline gluta-

© 2005 Scandinavian Physiological Society

mate level. However, the inhibition of glutamate transport actually decreased the baseline glutamate level (Figs 3 and 4), suggesting that spontaneous glutamate release rather than glutamate uptake had occurred under baseline conditions. The insertion of a dialysis probe inevitably damages the myocardium. Although we waited for 2 h after implantation of the dialysis probe and the glutamate level declined with time, glutamate release from damaged myocardium may have continued. Notwithstanding this limitation, we were able to detect glutamate release in response to acute myocardial ischaemia and inhibition of Na^+,K^+-ATPase. Therefore, our interpretation that glutamate release was dependent on the reverse transport of glutamate transporter may be reasonable.

Supplementing the heart with glutamate has been shown to have beneficial effect on the recovery of contractile function in post-surgical patients (Arsenian 1998). The myocardial interstitial glutamate level remained increased during 15-min reperfusion whereas the myocardial interstitial ACh level returned towards the baseline level. Although the reason for different responses upon reperfusion was unanswered in the present study, the sustained increase in the glutamate level may have therapeutic effect on its own.

In conclusion, acute myocardial ischaemia and inhibition of Na^+,K^+-ATPase did not increase myocardial interstitial choline level despite a significant increase in myocardial interstitial ACh level. By contrast, both interventions significantly increased the myocardial interstitial glutamate level. The glutamate transporter contributed to myocardial interstitial glutamate release via retrograde transport.

This study was supported by Health and Labour Sciences Research Grant for Research on Advanced Medical Technology (H14-Nano-002) from the Ministry of Health Labour and Welfare of Japan, by Grant-in-Aid for Scientific Research (C-15590786) from the Ministry of Education, Science, Sports and Culture of Japan, and by the Program for Promotion of Fundamental Studies in Health Science of the Organization for Pharmaceutical Safety and Research from Pharmaceuticals and Medical Devices Agency (PMDA).

References

Akiyama, T. & Yamazaki, T. 1999. Norepinephrine release from cardiac sympathetic nerve endings in the in vivo ischemic region. *J Cardiovasc Pharmacol* 34(Suppl. 4), S11–S14.

Akiyama, T., Yamazaki, T. & Ninomiya, I. 1991. In vivo monitoring of myocardial interstitial norepinephrine by dialysis technique. *Am J Physiol Heart Circ Physiol* 261, H1643–H1647.

Akiyama, T., Yamazaki, T. & Ninomiya, I. 1994. In vivo detection of endogenous acetylcholine release in cat ventricles. *Am J Physiol Heart Circ Physiol* 266, H854–H860.

Arsenian, M. 1998. Potential cardiovascular applications of glutamate, aspartate, and other amino acids. *Clin Cardiol* 21, 620–624.

Bäckström, T., Goiny, M., Lockowandt, U., Liska, J. & Franco-Cereceda, A. 2003. Cardiac outflow of amino acids and purines during myocardial ischemia and reperfusion. *J Appl Physiol* 94, 1122–1128.

Brühl, A., Hafner, G. & Löffelholz, K. 2004. Release of choline in the isolated heart, an indicator of ischemic phospholipid degradation and its protection by ischemic preconditioning: no evidence for a role of phospholipase D. *Life Sci* 75, 1609–1620.

Glantz, S.A. 2002. *Primer of Biostatistics*, 5th edn. McGraw-Hill, New York.

Hearse, D.J. 1979. Oxygen deprivation and early myocardial contractile failure: a reassessment of the possible role of adenosine triphosphate. *Am J Cardiol* 44, 1115–1121.

Kawada, T., Yamazaki, T., Akiyama, T. *et al.* 2000. Differential acetylcholine release mechanisms in the ischemic and non-ischemic myocardium. *J Mol Cell Cardiol* 32, 405–414.

Kawada, T., Yamazaki, T., Akiyama, T. *et al.* 2001a. Vagosympathetic interactions in ischemia-induced myocardial norepinephrine and acetylcholine release. *Am J Physiol Heart Circ Physiol* 280, H216–H221.

Kawada, T., Yamazaki, T., Akiyama, T. *et al.* 2001b. In vivo assessment of acetylcholine-releasing function at cardiac vagal nerve terminals. *Am J Physiol Heart Circ Physiol* 281, H139–H145.

Kawada, T., Yamazaki, T., Akiyama, T. *et al.* 2002. Disruption of vagal efferent axon and nerve terminal function in the postischemic myocardium. *Am J Physiol Heart Circ Physiol* 283, H2687–H2691.

Kennergren, C., Nyström, B., Nyström, U. *et al.* 1997. In situ detection of myocardial infarction in pig by measurements of aspartate aminotransferase (ASAT) activity in the interstitial fluid. *Scand Cardiovasc J* 31, 343–349.

Kennergren, C., Mantovani, V., Lönnroth, P., Nyström, B., Berglin, E. & Hamberger, A. 1999. Extracellular amino acids as markers of myocardial ischemia during cardioplegic heart arrest. *Cardiology* 91, 31–40.

Li, S., Jiang, Q., Stys, P.K. 2000. Important role of reverse Na^+-Ca^{2+} exchange in spinal cord white matter injury at physiological temperature. *J Neurophysiol* 84, 1116–1119.

Lockman, P.R. & Allen, D.D. 2002. The transport of choline. *Drug Dev Ind Pharm* 28, 749–771.

Mochizuki, S. & Jiang, C. 1998. Na^+/Ca^{++} exchanger and myocardial ischemia/reperfusion. *Jpn Heart J* 39, 707–714.

Nicholls, D.G. 1994. *Proteins, Transmitters and Synapses*, pp. 186–199. Blackwell Science, London.

Schömig, A., Dart, A.M., Dietz, R., Mayer, E. & Kübler, W. 1984. Release of endogenous catecholamines in the ischemic myocardium of the rat. Part A: Locally mediated release. *Circ Res* 55, 689–701.

Schömig, A., Kurz, T., Richardt, G. & Schömig, E. 1988. Neuronal sodium homeostasis and axoplasmic amine concentration determine calcium-independent noradrenaline release in normoxic and ischemic rat heart. *Circ Res* 63, 214–226.

© 2005 Scandinavian Physiological Society

Schwartz, J.H. 2000. Neurotransmitters. In: E.R. Kandel, J.H. Schwartz & T.M. Jessell (eds) *Principles of Neural Science*, 4th edn, pp. 280–297. McGraw-Hill, New York.

Song, D., O'Regan, M.H. & Phillis, J.W. 1996. Release of the excitotoxic amino acids, glutamate and aspartate, from the isolated ischemic/anoxic rat heart. *Neurosci Lett* 220, 1–4.

Yamazaki, T., Akiyama, T., Kitagawa, H., Takauchi, Y. & Kawada, T. 1996. Elevation of either axoplasmic norepinephrine or sodium level induced release of norepinephrine from cardiac sympathetic nerve terminals. *Brain Res* 737, 343–346.

Yamazaki, T., Akiyama, T., Kitagawa, H., Takauchi, Y., Kawada, T. & Sunagawa, K. 1997. A new, concise dialysis approach to assessment of cardiac sympathetic nerve terminal abnormalities. *Am J Physiol Heart Circ Physiol* 272, H1182–H1187.

Yamazaki, T., Akiyama, T. & Kawada, T. 1999. Effects of ouabain on in situ cardiac sympathetic nerve endings. *Neurochem Int* 35, 439–445.

© 2005 Scandinavian Physiological Society

Am J Physiol Heart Circ Physiol 289: H924–H930, 2005.
First published April 15, 2005; doi:10.1152/ajpheart.01207.2004.

Microdialysis separately monitors myocardial interstitial myoglobin during ischemia and reperfusion

Hirotoshi Kitagawa,[1] Toji Yamazaki,[2] Tsuyoshi Akiyama,[2]
Masaru Sugimachi,[3] Kenji Sunagawa,[4] and Hidezo Mori[2]

[1]*Department of Anesthesiology, Shiga University of Medical Science, Otsu; Departments of* [2]*Cardiac Physiology and* [3]*Cardiovascular Dynamics, National Cardiovascular Center Research Institute, Suita; and* [4]*Department of Cardiovascular Medicine, Kyushu University Graduate School of Medical Sciences, Fukuoka, Japan*

Submitted 1 December 2004; accepted in final form 6 April 2005

Kitagawa, Hirotoshi, Toji Yamazaki, Tsuyoshi Akiyama, Masaru Sugimachi, Kenji Sunagawa, and Hidezo Mori. Microdialysis separately monitors myocardial interstitial myoglobin during ischemia and reperfusion. *Am J Physiol Heart Circ Physiol* 289: H924–H930, 2005. First published April 15, 2005; doi:10.1152/ajpheart.01207.2004.—Direct monitoring of myoglobin efflux during ischemia and reperfusion has been limited because of inherent sample collection problems in the ischemic region. Recently, the cardiac dialysis technique has offered a powerful method for monitoring myocardial interstitial levels of low-molecular-weight compounds in the cardiac ischemic region. In the present study, we extended the molecular target to high-molecular-weight compounds by use of microdialysis probes with a high-molecular-mass cutoff and monitored myocardial interstitial myoglobin levels. A dialysis probe was implanted in the left ventricular free wall in anesthetized rabbits. The main coronary artery was occluded for 60 or 120 min. We examined the effects of myocardial ischemia and reperfusion on myocardial interstitial myoglobin levels. Interstitial myoglobin increased within 15 min of ischemia and continued to increase during 120 min of ischemia, whereas blood myoglobin increased at 45 min of ischemia. Lactate and myoglobin in the interstitial space increased during the same period. At 60 min of ischemia, reperfusion markedly accelerated interstitial myoglobin release. The interstitial myoglobin level was fivefold higher at 0–15 min of reperfusion than at 60–75 min of coronary occlusion. The dialysis technique permits earlier detection of myoglobin release and separately monitors myoglobin release during ischemia and reperfusion. Myocardial interstitial myoglobin levels can serve as an index of myocardial injury evoked by ischemia or reperfusion.

infarction; interstitial space; membrane permeability

IT IS WELL KNOWN that certain proteins, including myoglobin, called serum cardiac markers, are released into the bloodstream in large quantities from necrotic cardiac muscle cells after myocardial infarction (20, 26, 43). However, because direct samples from the ischemic region are not readily obtainable, in situ studies on efflux of these proteins in the cardiac ischemic region have been limited (22). This problem of sample collection from the ischemic region remains unresolved. First, it is uncertain exactly when cardiac markers appear from injured myocardium. The appearance of cardiac markers indicates the turning point from reversible injury to irreversible damage (43). However, the first appearance of cardiac markers in the bloodstream is influenced by the slow transport of cardiac markers from the interstitial space into the bloodstream (20). Thus the detection of this appearance is of great value in understanding the pathophysiological events induced by myocardial ischemia. Second, recent experimental and clinical findings suggest that reperfusion itself seems to accelerate the release of cardiac markers (18, 37, 38). However, the extent to which reperfusion contributes to relative changes in their release is unclear. To determine myocardial injury evoked by reperfusion, more information is needed about the extent to which ischemia and reperfusion affect changes in the release of cardiac markers. Third, present methods used to measure infarct size require tissue analysis several hours after the ischemic event (8). Furthermore, histochemical analysis depends on the times of ischemia and reperfusion (23, 33). Concise, dissociated assessments of ischemia and reperfusion injury have been a frequent object of research.

In general, mobilization of cardiac markers from ischemic myocardium to the bloodstream has been divided into two different sequences: release from the myocardial cell to the interstitial space and transport from the interstitial space into the bloodstream (20). Therefore, if we examine the first process in in situ myocardium, we can discuss the pathophysiological changes during development of ischemic myocardial necrosis. However, little information is available on interstitial protein kinetics in the ischemic region (15). Examination of protein kinetics in the ischemic region has been limited to assessment of protein kinetics in the isolated Langendorff-perfused heart (28, 39). Recently, a cardiac dialysis technique has provided a powerful method for monitoring myocardial interstitial levels of low-molecular-weight compounds in the cardiac ischemic region (2, 6, 14, 31). Furthermore, this method is suitable for distinguishing between ischemia and reperfusion responses (32). By improving the microdialysis probes with a high-molecular-mass cutoff membrane, we have extended the molecular target to high-molecular-weight peptides and proteins and monitored myocardial interstitial protein levels.

In the present study, we chose myoglobin as one of the earliest biochemical markers in myocardial injury (4, 34). We applied the dialysis technique to the heart of anesthetized rabbits and investigated myocardial interstitial myoglobin levels during coronary occlusion and reperfusion. To address the above-mentioned issues, we compared the first appearance of myocardial interstitial myoglobin levels with that of low-molecular-weight metabolites (lactate and glycerol). Further-

Address for reprint requests and other correspondence: T. Yamazaki, Dept. of Cardiac Physiology, National Cardiovascular Center Research Institute, 5-7-1 Fujishirodai, Suita, Osaka 565-8565, Japan (E-mail: yamazaki@ri.ncvc.go.jp).

The costs of publication of this article were defrayed in part by the payment of page charges. The article must therefore be hereby marked "*advertisement*" in accordance with 18 U.S.C. Section 1734 solely to indicate this fact.

0363-6135/05 $8.00 Copyright © 2005 the American Physiological Society

more, we compared the time course of myocardial interstitial myoglobin during reperfusion after ischemia with that of sustained ischemia and examined the changes in myoglobin release evoked by reperfusion. The results of the present study indicate that microdialysis is suitable for distinguishing between ischemia and reperfusion injury.

MATERIALS AND METHODS

Animal Preparation

The investigation conformed with the *Guide for the Care and Use of Laboratory Animals* published by the National Institutes of Health (NIH Publication No. 85-23, Revised 1996). All protocols were approved by the Animal Subjects Committee of the National Cardiovascular Center. Thirty adult male Japanese White rabbits (2.5–3.2 kg) were anesthetized with pentobarbital sodium (30–35 mg/kg iv). The level of anesthesia was maintained with a continuous intravenous infusion of pentobarbital sodium (1–2 $mg \cdot kg^{-1} \cdot h^{-1}$). The rabbits were intubated and ventilated with room air mixed with oxygen. Body temperature was maintained at ~39°C with a heating pad and lamp. Heart rate (HR), mean arterial pressure (MAP), and electrocardiogram were monitored and recorded continuously. Heparin sodium (200 IU/kg) was first administered intravenously and then maintained with a continuous infusion (5–10 $IU \cdot kg^{-1} \cdot h^{-1}$) to prevent blood coagulation. With the animal in the lateral position, the fifth or sixth rib on the left side was partially removed to expose the heart. A small incision was made in the pericardium, and the dialysis probe was implanted in the region perfused by the left circumflex coronary artery (LCX) of the left ventricular wall. A snare was placed around the main branch of the LCX to act as the occluder for later coronary occlusion. To ensure that the sampling area was in the ischemic region, we examined the color and motion of the ventricular wall during a brief occlusion and confirmed that the dialysis probe was correctly located. To avoid a preconditioning effect, the duration of occlusion was limited to a few seconds.

Dialysis Technique

We designed a handmade long transverse dialysis probe (1). One end of a polyethylene tube (25 cm long, 0.5 mm OD, 0.2 mm ID) was dilated with a 27-gauge needle (0.4 mm OD). Each end of the dialysis fiber (8 mm long, 0.215 mm OD, 0.175 mm ID, 300 Å pore size; Evaflux type 5A, Kuraray Medical) was inserted into the polyethylene tube and glued. A fine guiding needle (25 mm long, 0.51 mm OD, 0.25 mm ID) was used for implantation of the dialysis probes. A guiding needle was connected to the dialysis probe with a stainless steel rod (5 mm long, 0.25 mm OD). At a perfusion speed of 5 μl/min, the in vitro recovery rate (RR) of myoglobin was 15 ± 0.6% (number of dialysis probes = 3). In vitro RR was defined as follows: $RR = (C_{in} - C_{out})/C_{in}$, where C_{in} and C_{out} are the concentrations of myoglobin in the perfusate and in the dialysate, respectively (19). For monitoring myocardial interstitial lactate and glycerol levels, we used a conventional dialysis fiber (PAN-1200, Asahi Chemical Japan) to detect low-molecular-weight compounds (1).

Dialysis probes were perfused with Ringer solution (in mM: 147.0 NaCl, 4.0 KCl, and 2.25 $CaCl_2$) at 5 μl/min using a microinjection pump (model CMA/100, Carnegie Medicine). Figure 1 shows the time course of dialysate myoglobin levels collected at 1-h intervals over a 4-h period after probe implantation. Dialysate myoglobin rapidly decreased to 261 ± 56 ng/ml at 2 h after probe implantation. Thereafter, it gradually decreased, reaching an almost steady level of 222 ± 37 ng/ml 4 h after probe implantation. On the basis of the results of this experiment, in the subsequent protocol, we discarded the first 120-min collections of dialysate and measured the dialysate myoglobin level twice at 30-min intervals. When dialysate myoglobin levels reached the steady level, we started the experimental protocol.

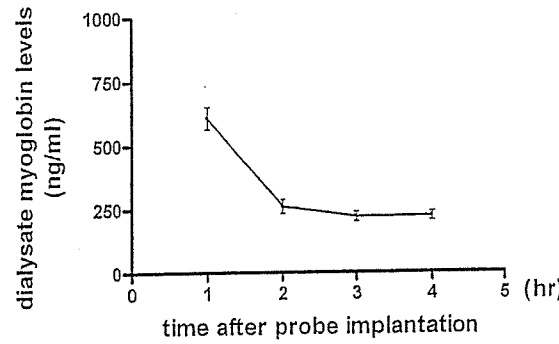

Fig. 1. Time course of dialysate myoglobin levels after probe implantation. Dialysate myoglobin levels decreased over the first 2 h and then reached an almost steady level. Values are means ± SE from 5 rabbits.

Sampling periods were 15 min (1 sampling volume = 75 μl) in control and during occlusion and reperfusion. Taking into consideration the dead space between the dialysis fiber and sample tube, we sampled the dialysate.

Dialysate myoglobin concentrations were measured as an index of myocardial interstitial myoglobin levels. Blood samples were obtained from the femoral artery. Using immunochemistry (Cardiac Reader, Roche Diagnostics), we measured the myoglobin levels (7). The detection limit of myoglobin was 30 ng/ml. The dialysate lactate and glycerol levels were measured by kinetic enzymatic analysis (CMA 600 analyzer, Carnegie Medicine) (30).

Experimental Protocols

After control sampling, we occluded the main branch of the LCX for 60 min and then released the occluder. We continuously sampled the dialysate from the ischemic region during 60 min of coronary occlusion and reperfusion.

Time course of dialysate lactate, glycerol, and myoglobin levels during myocardial ischemia. We compared the dialysate myoglobin levels with the blood myoglobin levels. After control sampling, we observed the time course of dialysate and blood myoglobin levels during 60 min of coronary occlusion. In addition, we measured simultaneously dialysate lactate and glycerol levels from the ischemic region in separate rabbits.

Time course of dialysate myoglobin levels during 60 min of reperfusion following 60 and 120 min of ischemia. Reperfusion modulates myocardial membrane damage and may accelerate dialysate myoglobin levels (18, 21, 37). We compared the time course of dialysate myoglobin during 60 min of reperfusion following 60 min of ischemia with that of 120 min of ischemia.

Time course of dialysate myoglobin levels during local administration of cyanide. To confirm whether the dialysate myoglobin level reflects myocardial damage evoked by ischemia or hypoxia, we tested the effect of local sodium cyanide (NaCN) administration on dialysate myoglobin levels. We collected a control dialysis sample and then replaced the perfusate with Ringer solution containing NaCN (30 mM), thereby locally administering NaCN for 60 min. We obtained four consecutive dialysate samples and measured the dialysate myoglobin levels.

At the end of each experiment, the rabbits were killed with an overdose of pentobarbital sodium, and the implant regions were checked to confirm that the dialysis probes had been implanted within the cardiac muscle.

Statistical Analysis

Dialysate lactate, glycerol, and myoglobin responses to coronary occlusion were statistically analyzed by one-way analysis of variance with repeated measures. When a statistically significant effect of

Table 1. *Changes in HR and MAP in coronary artery occlusion*

	120 min Coronary Occlusion								
	C	5	15	30	45	60	75	90	105
HR, beats/min	268±7	264±8	242±8*	250±3*	253±4*	252±4*	250±4*	251±3*	248±4*
MAP, mmHg	84±4	74±5*	69±5*	71±5*	68±5*	67±5*	66±4*	65±4*	64±5*
	60 min Occlusion - 60 min Reperfusion								
	C	5	15	30	45	R5	R15	R30	R45
HR, beats/min	274±9	261±6*	255±7*	254±6*	261±7*	256±5*	263±10*	264±12*	263±9*
MAP, mmHg	78±4	67±3*	65±2*	67±2*	65±2*	61±2*	60±3*†	61±2*	58±2*†

Values are mean ± SE. Data were obtained during control (C), after 5, 15, 30, 45, 60, 75, 90, and 105 min of coronary artery occlusion, and after 5, 15, 30, and 45 min of reperfusion (R). *$P < 0.05$ vs. control. †$P < 0.05$ vs. 45 min occlusion.

coronary occlusion was detected as a whole, the Newman-Keuls test was applied to determine which mean values differed significantly from each other (40). Statistical significance was defined as $P < 0.05$. Values are means ± SE.

RESULTS

Time Course of HR and MAP

Table 1 shows the time courses of HR and MAP during coronary occlusion and reperfusion. Coronary occlusion decreased HR and MAP. Reperfusion did not alter HR but temporarily decreased MAP.

Time Course of Dialysate Lactate, Glycerol, and Myoglobin Levels During Myocardial Ischemia

Coronary occlusion significantly altered dialysate myoglobin levels (Fig. 2). Dialysate myoglobin levels increased significantly from 168 ± 32 ng/ml in the control to 570 ± 107 ng/ml at 0–15 min of occlusion. During 60 min of coronary occlusion, dialysate myoglobin levels progressively increased and reached 2,583 ± 208 ng/ml at 45–60 min of occlusion. A significant increase in blood myoglobin occurred at 45–60 min of coronary occlusion. Dialysate lactate levels were 1.00 ± 0.21 mmol/l in the control and increased after coronary occlusion (Fig. 3). During 60 min of coronary occlusion, dialysate lactate levels markedly increased and reached 3.34 ± 0.50 mmol/l at 45–60 min of occlusion. During 60 min of coronary occlusion, dialysate glycerol levels also increased and reached 232 ± 33 μmol/l at 45–60 min of occlusion.

Time Course of Dialysate Myoglobin Levels During 60 min of Reperfusion Following 60 and 120 Minutes of Ischemia

There were no significant differences in the control dialysate myoglobin levels between the two groups (Fig. 4). During ischemia, the dialysate myoglobin levels progressively increased and reached 4,054 ± 659 ng/ml at 105–120 min of coronary occlusion. During 60 min of coronary occlusion, there were no statistically significant differences in the dialysate myoglobin levels between the two groups. After release of the occluder, the dialysate myoglobin levels markedly increased to 12,569 ± 2,347 ng/ml at 0–15 min of reperfusion. The dialysate myoglobin levels at 0–15 min of reperfusion were fivefold higher than those at 60–75 min of 120 min of coronary occlusion. Furthermore, these values were higher than peak levels during 120 min of coronary occlusion. The

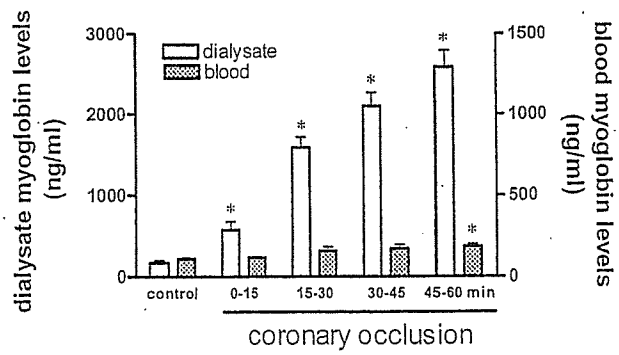

Fig. 2. Time courses of dialysate and blood myoglobin levels during 60 min of ischemia. Values are means ± SE. *$P < 0.05$ vs. control.

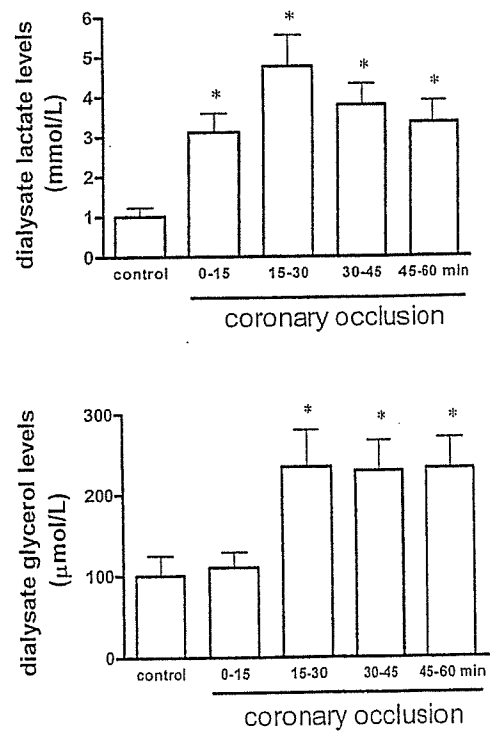

Fig. 3. Time courses of dialysate lactate (*top*) and glycerol (*bottom*) levels during 60 min of ischemia. Values are means ± SE. *$P < 0.05$ vs. control.

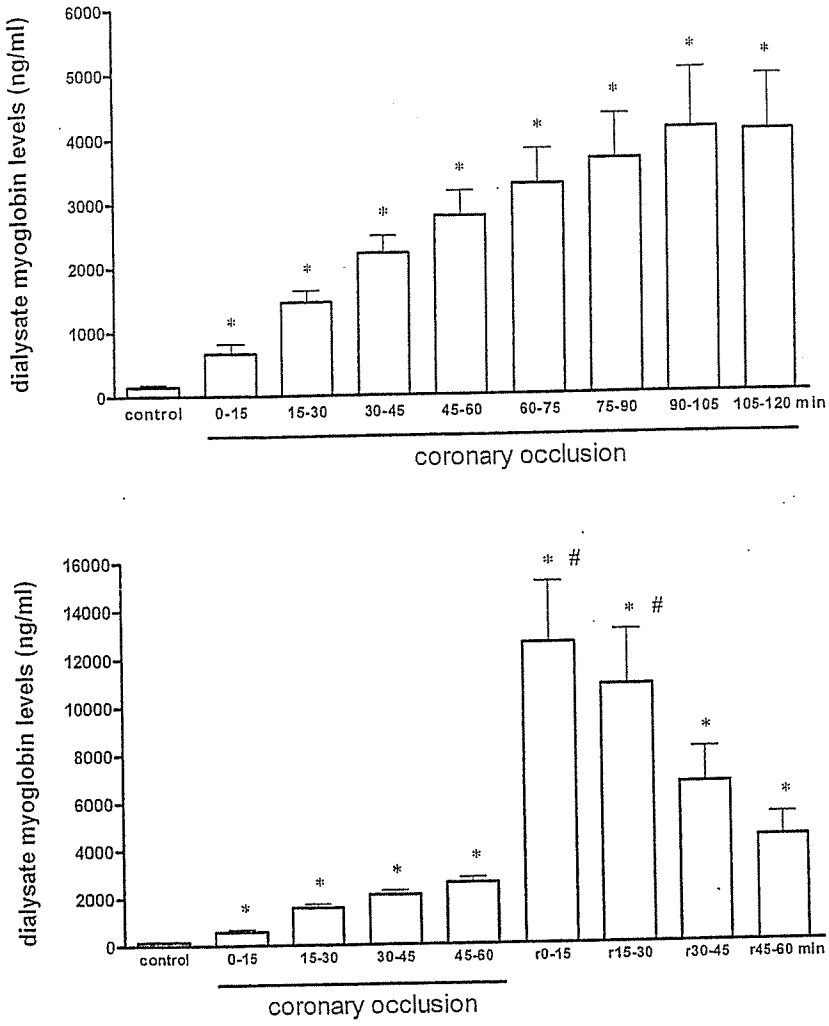

Fig. 4. Time courses of dialysate myoglobin levels during 120 min of ischemia (*top*) and 60 min of ischemia followed by 60 min of reperfusion (r, *bottom*). Values are means ± SE. $^{*}P < 0.05$ vs. control. $^{\#}P < 0.05$ vs. 45–60 min of occlusion.

dialysate myoglobin levels gradually decreased and reached 4,391 ± 879 ng/ml at 45–60 of reperfusion. At 0–15 min of reperfusion, dialysate lactate and glycerol levels were 3.27 ± 0.61 mmol/l and 242 ± 37.7 μmol/l, respectively. Dialysate lactate and glycerol levels remained unchanged at 0–15 min of reperfusion.

Time Course of Dialysate Myoglobin Levels During Local Administration of NaCN

Local administration of NaCN increased the dialysate myoglobin levels (Fig. 5). This increase was statistically significant compared with the control level at all collection periods during NaCN administration, except at 0–15 min. The maximum myoglobin level was comparable to that observed during 60 min of ischemia.

DISCUSSION

Using the dialysis technique in the in vivo rabbit heart, we observed myocardial interstitial myoglobin levels during myocardial ischemia and reperfusion. Our data demonstrated myoglobin release in the early stage of cardiac ischemia and its enhancement by reperfusion. We discuss here the time course of myocardial myoglobin release during coronary occlusion and after reperfusion.

We show for the first time that myoglobin release increases within 15 min of ischemia and continues to increase during 60 min of ischemia. However, significant changes in the blood myoglobin level occurred at 45–60 min of coronary occlusion. Our data suggest a contrast between blood and dialysate

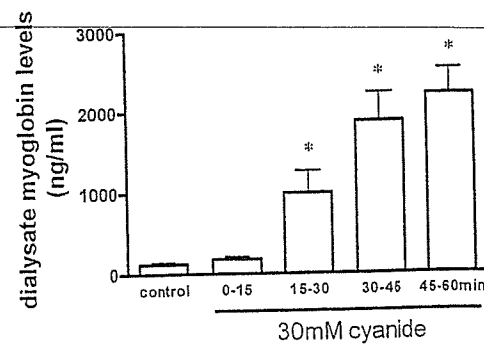

Fig. 5. Time course of dialysate myoglobin levels during local administration of sodium cyanide (30 mM). Values are means ± SE. $^{*}P < 0.05$ vs. control.

myoglobin levels during ischemia. The delay of the first appearance of myoglobin in the bloodstream is mainly due to the slow transport of myoglobin from the interstitial space into the bloodstream (20). Therefore, myoglobin concentration measured by cardiac microdialysis provides information regarding early release of cytosol protein into the interstitial space. Within the 15-min time resolution, this increase in myoglobin release was accompanied by increases in interstitial lactate. Dead space volume between the dialysis fiber and the sample microtube was identical for lactate, glycerol, and myoglobin. The currently accepted concept (20) is that leakage of anaerobic metabolites precedes macromolecular protein release during ischemia. Anaerobic metabolites accumulate and leak from the ischemic region within minutes via diffusion or transport (6, 12, 41). In contrast to low-molecular-weight metabolites, macromolecular proteins could be released into the interstitial space without cytosol accumulation of myoglobin, probably via bleb or altered permeability. Although sampling periods of 15 min are too long to enable us to distinguish the rate of release of lactate vs. myoglobin, our data at least suggest that cellular metabolic derangement is involved in membrane disruption for myoglobin release.

Myocardial injury caused by ischemia-reperfusion is associated with membrane phospholipid degradation, which is thought to underlie disruption of the cell membrane (27). Glycerol is an end product of membrane phospholipid degradation and has been used to study membrane phospholipid degradation after cerebral ischemia and seizures (12). In the present study, dialysate glycerol was examined as a potential marker for membrane phospholipid degradation in myocardial ischemia and reperfusion. We observed increases in dialysate glycerol levels during 15–60 min of ischemia but not during reperfusion. In general, phospholipid degradation is accentuated during reperfusion (27). Therefore, dialysate glycerol is not suitable as an index of membrane phospholipid degradation, and the release of glycerol from membrane phospholipid degradation might be too small to allow detection in blood-perfused heart.

Early change of cytosol myoglobin was detected by immunofluorescence after occlusion of the coronary artery (16, 25). Histochemical studies demonstrated that intracellular diffusion of cytosol myoglobin into the nuclei and mitochondria was evident as early as 0.5 h after coronary artery occlusion (17, 25). Our data demonstrate early loss of cytosol myoglobin into the interstitial space. Release of cytosol protein is caused by membrane damage via alteration of permeability or bleb formation. Blebs appeared on the cell surfaces, and the cell began to swell within 10–20 min of ATP depletion in a glia cell line or hepatocytes (13, 24). Furthermore, NMR spectroscopy suggested that sarcolemmal membranes are gradually permeabilized to large molecules by ischemia (3). These alterations of sarcolemmal membranes might be involved in early release of myoglobin during the myocardial ischemia. Our method offers extremely fast and sensitive analysis of membrane injury in myocardial ischemia that is not evident by histological or blood analysis. Quantitative assessment of interstitial myoglobin levels could be performed independently of reperfusion cell injury and could be helpful in devising various myocardial preservation treatments.

We show that reperfusion markedly accelerates myoglobin release in the ischemic region. The interstitial myoglobin levels at 0–15 min of reperfusion were fivefold higher than those at 60–75 min of 120 min of coronary occlusion. During the reperfusion period, interstitial accumulated myoglobin might be washed out into the bloodstream (37). Therefore, the amount of released myoglobin at reperfusion could be markedly greater than the changes in interstitial myoglobin concentrations at reperfusion. Release of cytosolic protein resulted from a disruption of a sarcolemmal bleb or an enhancement of membrane permeability (5, 29, 35). Either condition may gain relevance during the reperfusion period. Thus the release of myoglobin during the reperfusion seems to serve as an index of disrupted sarcolemmal membrane.

Although the exact mechanisms of accelerated myoglobin release cannot be determined from the present study, our data suggest that substances induced during reperfusion differ from those induced during ischemia. Reperfusion enhanced myoglobin release but did not accelerate lactate or glycerol release in the interstitial space, whereas ischemia accompanied macromolecular myoglobin release as well as anaerobic metabolite release. Furthermore, in the previous studies, neither catecholamine nor acetylcholine release was accelerated by reperfusion in ischemic cardiac sympathetic and parasympathetic nerve endings (2, 14). During reperfusion, surviving myocardial cells and nerve terminals quickly recover aerobic metabolism and take up these accumulated substances, whereas myocardial cells have no capability of myoglobin uptake via the sarcolemmal membrane, leading to continued myoglobin release via the disrupted membrane. Reperfusion may enhance membrane permeability (5). Further disruption of membrane blebs may cause rupture of the membrane (29, 35). Alternatively, in isolated perfused rats, leakage of cytoplasmic enzymes during reoxygenation is accelerated by cardiac revived beating, because the cell membrane becomes fragile during the preceding anoxia (36). In either condition, reperfusion-induced breakdown of membrane phospholipids contributes to an alteration of permeability or bleb formation (27). Disruption of the membrane phospholipid bilayer is likely to play a role in myoglobin release from the cyotosome into the interstitial spaces.

In the present study, we demonstrate that loss of cytosol myoglobin occurs during myocardial ischemia and reperfusion and might be involved in the outcome and pathophysiology of the ischemic heart. Loss of cytosol myoglobin may precede, at least in part, histological evidence of necrosis and occur in the remaining viable myocardium that is not necrotic (11). In vertebrate heart, myoglobin is involved in the transport of oxygen from the sarcolemma to the mitochondria (42). Recent studies from myoglobin knockout mice indicate that myoglobin contributes to the scavenging of bioactive nitric oxide (NO) or oxygen radicals during ischemia-reperfusion (9, 10). NO production and/or oxidant injury occur during the reperfusion period. In hearts lacking myoglobin, changes in NO and oxidative stress have a much larger impact on the maintenance of vascular tone and cardiac function (44). Similarly, in myoglobin knockout mice, loss of cytosol myoglobin may be involved in the delayed restoration of cardiac contractility in the postischemic region.

There are several limitations to the present study. First, with application of the dialysis technique to the heart, we had to perform this experiment as an acute surgical preparation. Probe implantation and/or surgical preparation might affect the con-

centration of myocardial interstitial myoglobin. To examine the effect of probe implantation and/or surgery, we performed the preliminary experiment on brief occlusion (3 min). Three minutes of coronary occlusion did not alter dialysate myoglobin levels. Furthermore, to confirm whether the dialysate myoglobin level reflects myocardial damage evoked by ischemia or hypoxia, we tested the effect of local NaCN administration on dialysate myoglobin levels: with NaCN, we found increases in dialysate myoglobin levels similar to the increase evoked by myocardial ischemia. Therefore, we believe that dialysate myoglobin levels reflect the release of myoglobin evoked by ischemia as well as by chemical hypoxia. The absolute myoglobin level might be affected by implantation and/or surgical preparation. However, it is possible to estimate myoglobin release from relative changes in myoglobin levels.

Second, in the present study, myocardial interstitial myoglobin levels during coronary occlusion and reperfusion were determined regionally. We implanted the dialysis probe in the midwall of the left ventricle. When the dialysis probe was implanted in the subendocardial zone, it is likely that subendocardial ischemia was much more severe than in the midwall, where the sampling was performed. Actually, subendocardial lactate was significantly greater than epicardial lactate during severe ischemia in the anesthetized dogs (6). Further studies are warranted concerning the influence of the ischemic area (subendocardial or marginal zone) on its myocardial interstitial myoglobin levels.

In summary, this microdialysis study in an ischemic animal model shows that coronary occlusion induced myoglobin release in minutes. Micromolecular metabolite (lactate) and macromolecular protein (myoglobin) increased during the first 15 min of ischemia. Reperfusion markedly enhanced myoglobin release without increases in lactate or glycerol levels. Elevation of myoglobin release represents an increase in sarcolemmal permeability or bleb formation during ischemia and reperfusion. Massive disruption of myocardial membrane occurs immediately after ischemia and is markedly accelerated by reperfusion. The dialysis technique permits more concise in vivo monitoring of myocardial membrane disruption during ischemia and reperfusion separately.

GRANTS

This study was supported by the Program for Promotion of Fundamental Studies in Health Science of the Organization for Pharmaceutical Safety and Research by grants-in-aid for scientific research from the Ministry of Education, Science.

REFERENCES

1. **Akiyama T, Yamazaki T, and Ninomiya I.** In vivo monitoring of myocardial interstitial norepinephrine by dialysis technique. *Am J Physiol Heart Circ Physiol* 261: H1643–H1647, 1991.
2. **Akiyama T, Yamazaki T, and Ninomiya I.** Differential regional response of myocardial interstitial noradrenaline levels to coronary occlusion. *Cardiovasc Res* 27: 817–822, 1993.
3. **Askenasy N, Vivi A, Tassini M, Navon G, and Farkas DL.** NMR spectroscopic characterization of sarcolemmal permeability during myocardial ischemia and reperfusion. *J Mol Cell Cardiol* 33: 1421–1433, 2001.
4. **Block MI, Said JW, Siegel RJ, and Fishbein MC.** Myocardial myoglobin following coronary artery occlusion. An immunohistochemical study. *Am J Pathol* 111: 374–379, 1983.
5. **Camilleri JP, Joseph D, Amat D, and Fabiani JN.** Impaired sacrolemmal membrane permeability in reperfused ischemic myocardium. Ultrastructual tracer study. *Virchows Arch* 388: 69–76, 1980.
6. **Delyani JA and Van Wylen GDL.** Endocardial and epicardial interstitial purines and lactate during graded ischemia. *Am J Physiol Heart Circ Physiol* 266: H1019–H1026, 1994.
7. **Dominici R, Infusino I, Valente C, Moraschineli I, and Franzini C.** Plasma or serum samples: measurements of cardiac troponin T and of other analytes compared. *Clin Chem Lab Med* 42: 945–951, 2004.
8. **Farb A, Kolodgie FD, Jones RM, Jenkins M, and Virmani R.** Early detection and measurement of experimental myocardial infarcts with horseradish peroxidase. *J Mol Cell Cardiol* 25: 343–353, 1993.
9. **Flögel U, Gödecke A, Klotz LO, and Schrader J.** Role of myoglobin in the antioxidant defense of the heart. *FASEB J* 18: 1156–1158, 2004.
10. **Flögel U, Merx MW, Gödecke A, Decking UKM, and Schrader J.** Myoglobin: a scavenger of bioactive NO. *Proc Natl Acad Sci USA* 98: 735–740, 2001.
11. **Heyndrickx GR, Amano J, Kenna T, Fallon JT, Patrick TA, Manders WT, Rogers GG, Rosendorff C, and Vatner SF.** Creatine kinase release not associated with myocardial necrosis after short periods of coronary artery occlusion in conscious baboons. *J Am Coll Cardiol* 6: 1299–1303, 1985.
12. **Hillered L, Valtysson J, Enblad P, and Persson L.** Interstitial glycerol as a marker for membrane phospholipid degradation in the acutely injured human brain. *J Neurol Neurosurg Psychiatry* 64: 486–491, 1998.
13. **Jurkowitz-Alexander MS, Altschuld RA, Hohl CM, Johnson JD, McDonald JS, Simmonds TD, and Horrocks LA.** Cell swelling, blebbing, and death are dependent on ATP depletion and independent of calcium during chemical hypoxia in a glial cell line (ROC-1). *J Neuorchem* 59: 344–352, 1992.
14. **Kawada T, Yamazaki T, Akiyama T, Sato T, Shishido T, Inagaki M, Sugimachi M, and Sunagawa K.** Differential acetylcholine release mechanisms in the ischemic and non-ischemic myocardium. *J Mol Cell Cardiol* 32: 405–414, 2000.
15. **Kennergren C, Nyström B, Nyström U, Berglin E, Larsson G, Mantovani V, Lönnroth P, and Hamberger A.** In situ detection of myocardial infarction in pig by measurements of asparate aminotransferase (ASAT) activity in the interstitial fluid. *Scand Cardiovasc J* 31: 343–349, 1997.
16. **Kent SP.** Diffusion of myoglobin in the diagnosis of early myocardial ischemia. *Lab Invest* 46: 265–270, 1982.
17. **Kent SP.** Intracellular diffusion of myoglobin. A manifestation of early cell injury in myocardial ischemia in dogs. *Arch Pathol Lab Med* 108: 827–830, 1984.
18. **Laperche T, Steg PG, Dehoux M, Benessiano J, Grollier G, Aliot E, Mossard JM, Aubry P, Coisne D, Hanssen M, and Iliou MC.** A study of biochemical markers of reperfusion early after thrombolysis for acute myocardial infarction. The PERM Study Group Prospective Evaluation of Reperfusion Markers. *Circulation* 92: 2079–2088, 1995.
19. **Le Quellec A, Dupin S, Genissel P, Savin S, Marchand B, and Houin G.** Microdialysis probes calibration: gradient and tissue dependent changes in no net flux and reverse dialysis methods. *J Pharmacol Toxicol Methods* 33: 11–16, 1995.
20. **Mair J.** Tissue release of cardiac markers: from physiology to clinical applications. *Clin Chem Lab Med* 37: 1077–1084, 1999.
21. **Matsumura K, Jeremy RW, Schaper J, and Becker LC.** Progression of myocardial necrosis during reperfusion of ischemic myocardium. *Circulation* 97: 795–804, 1998.
22. **Miura T.** Does reperfusion induce myocardial necrosis? *Circulation* 82: 1070–1072, 1990.
23. **Nachlas MM and Shnitka TK.** Macroscopic identification of early myocardial infarcts by alterations in dehydrogenase activity. *Am J Pathol* 42: 379–405, 1963.
24. **Nieminen AL, Gores GJ, Wray BE, Tanaka Y, Herman B, and Lemasters JJ.** Calcium dependence of bleb formation and cell death in hepatocytes. *Cell Calcium* 9: 237–246, 1988.
25. **Nomoto K, Mori N, Miyamoto J, Shoji T, and Nakamura K.** Relationship between sarcolemmal damage and appearance of amorphous matrix densities in mitochondria following occlusion of coronary artery in rats. *Exp Mol Pathol* 51: 231–242, 1989.
26. **Ortmann C, Pfeiffer H, and Brinkmann B.** A comparative study on the immunohistochemical detection of early myocardial damage. *Int J Legal Med* 113: 215–220, 2000.
27. **Prasad MR, Popescu LM, Moraru II, Liu X, Maity S, Engelman RM, and Das DK.** Role of phospholipases A_2 and C in myocardial ischemic reperfusion injury. *Am J Physiol Heart Circ Physiol* 260: H877–H883, 1991.

28. Remppis A, Scheffold T, Greten J, Haass M, Greten T, Kubler W, and Katus HA. Intracellular compartmentation of troponin T: release kinetics after global ischemia and calcium paradox in the isolated perfused rat heart. *J Mol Cell Cardiol* 27: 793–803, 1995.
29. Sage MD and Jennings RB. Cytoskeletal injury and subsarcolemmal bleb formation in dog heart during in vitro total ischemia. *Am J Pathol* 133: 327–337, 1988.
30. Sarrafzadeh AS, Sakowitz OW, Kiening KL, Benndorf G, Lanksch WR, and Unterberg AW. Bedside microdialysis: a tool to monitor cerebral metabolism in subarachnoid hemorrhage patients? *Crit Care Med* 30: 1062–1070, 2002.
31. Shindo T, Akiyama T, Yamazaki T, and Ninomiya I. Increase in myocardial norepinephrine during a short period of coronary occlusion. *J Auton Nerv Syst* 48: 91–96, 1994.
32. Shindo T, Akiyama T, Yamazaki T, and Ninomiya I. Regional myocardial interstitial norepinephrine kinetics during coronary occlusion and reperfusion. *Am J Physiol Heart Circ Physiol* 270: H245–H251, 1996.
33. Shirato C, Miura T, Ooiwa H, Toyofuku T, Wilborn WH, and Downey JM. Tetrazolium artifactually indicates superoxide dismutase-induced salvage in reperfused rabbit heart. *J Mol Cell Cardiol* 21: 1187–1193, 1989.
34. Spangenthal EJ and Ellis AK. Cardiac and skeletal muscle myoglobin release after reperfusion of injured myocardium in dogs with systemic hypotension. *Circulation* 91: 2635–2641, 1995.
35. Steenbergen C, Hill ML, and Jennings RB. Volume regulation and plasma membrane injury in aerobic, anaerobic, and ischemic myocardium in vitro. Effects of osmotic cell swelling on plasma membrane integrity. *Circ Res* 57: 864–875, 1985.
36. Takami H, Matsuda H, Kuki S, Nishimura M, Kawashima Y, Watari H, Furuya E, and Tagawa K. Leakage of cytoplasmic enzymes from rat heart by the stress of cardiac beating after increase in cell membrane fragility by anoxia. *Pflügers Arch* 416: 144–150, 1990.
37. Van der Laarse A, van der Wall EE, van den Pol RC, Vermeer F, Verheugt FW, Krauss XH, Bar FW, Hermens WT, Willems GW, and Simoons ML. Rapid enzyme release from acutely infarcted myocardium after early thrombolytic therapy: washout or reperfusion damage? *Am Heart J* 115: 711–716, 1988.
38. Van Kreel BK, van den Veen FH, Willems GM, and Hermens WT. Circulatory models in assessment of cardiac enzyme release in dogs. *Am J Physiol Heart Circ Physiol* 264: H747–H757, 1993.
39. Van Nieuwenhoven FA, Musters RJ, Post JA, Verkleij AJ, Van der Vusse GJ, and Glatz JF. Release of proteins from isolated neonatal rat cardiomyocytes subjected to simulated ischemia or metabolic inhibition is independent of molecular mass. *J Mol Cell Cardiol* 28: 1429–1434, 1996.
40. Wiener BJ. *Statistical Principles in Experimental Design* (2nd ed.). New York: McGraw-Hill, 1971.
41. Wikström G, Ronquist G, Nilsson S, Maripu E, and Waldenström A. Continuous monitoring of energy metabolites using microdialysis during myocardial ischaemia in the pig. *Eur Heart J* 16: 339–347, 1995.
42. Wittenberg JB and Wittenberg BA. Myoglobin function reassessed. *J Exp Biol* 206: 2011–2020, 2003.
43. Wu AH. Biochemical markers of cardiac damage: from traditional enzymes to cardiac-specific proteins. IFCC Subcommittee on Standardization of Cardiac Markers (S-SCM). *Scand J Clin Lab Invest Suppl* 230: 74–82, 1999.
44. Wunderlich C, Flögel U, Gödecke A, Heger J, and Schrader J. Acute inhibition of myoglobin impairs contractility and energy state of iNOS-overexpressing hearts. *Circ Res* 92: 1352–1358, 2003.

GASTROENTEROLOGY 2005;129:577-590

Oncogenic Potential of MEK1 in Rat Intestinal Epithelial Cells Is Mediated via Cyclooxygenase-2

KOGA KOMATSU,*,† F. GREGORY BUCHANAN,* SHARADA KATKURI,* JASON D. MORROW,§ HIROYASU INOUE,‖ MICHIRO OTAKA,† SUMIO WATANABE,† and RAYMOND N. DuBOIS*

*Departments of Cell/Developmental Biology, Cancer Biology, and Medicine, Vanderbilt-Ingram Cancer Center, Nashville, Tennessee; †Department of Gastroenterology, Akita University School of Medicine, Akita, Japan; §Department of Pharmacology and Medicine, Vanderbilt University Medical Center, Nashville, Tennessee; and ‖Department of Pharmacology, National Cardiovascular Center Research Institute, Osaka, Japan

Background & Aims: The mitogen-activated protein kinase/extracellular signal–regulated protein kinase kinase (MEK) pathway plays an important role in the regulation of cell growth and differentiation. Constitutively active components of the MEK signaling cascade can induce oncogenic transformation in many cell systems. Downstream MEK signaling also plays an important role in the regulation of cyclooxygenase-2 (COX-2), which is known to be involved in colorectal cancer. Therefore, we determined the role of COX-2 on the oncogenic potential of MEK1 in nontransformed rat intestinal epithelial cells. *Methods:* Constitutively active MEK1 (CA-MEK) mutant transfected rat intestinal epithelial cells were established and tested for their ability to grow in soft agar and form tumors in vivo. The effect of CA-MEK on sodium butyrate (NaB)–induced apoptosis was evaluated by the Annexin V assay. The transcriptional activity and posttranscriptional stability of the *COX-2* gene was determined by transient transfection with COX-2 reporter variants and by Northern analysis. To address the role of COX-2 in tumor growth in vivo, xenografted mice were treated with celecoxib (100 mg/kg) or vehicle. *Results:* CA-MEK transfected RIE-1 and IEC-6 cells formed colonies in soft agar and tumors in nude mice. These cells showed resistance to NaB-induced apoptosis and cell cycle arrest. MEK activation led to increased expression of COX-2, Bcl-X_L, Mcl-1, and phosphorylated Bad and decreased expression of Bak. Along with elevated COX-2 levels, PGI_2 and PGE_2 levels were also increased. Pharmacologic inhibition of COX-2 inhibited MEK-induced tumor growth in vivo through enhanced apoptosis. *Conclusions:* COX-2 and its bioactive lipid products may play an important role in MEK-induced transformation.

Escape from cell differentiation and programmed cell death provides a distinct survival advantage for transformed cells.[1] Cell growth, differentiation, and apoptosis are controlled by a wide variety of extracellular signals, many of which induce mitogen-activated protein kinases (MAPKs).[2–4] MAPKs are serine-threonine kinases that are activated by phosphorylation of specific amino acids in response to extracellular stimuli. The first member of this family to be characterized was the extracellular signal–regulated protein kinase (ERK), which is phosphorylated and activated by MAPK/ERK kinase (MEK).[2,5]

In normal intestinal mucosa, cell growth, differentiation, and apoptosis are important homeostatic mechanisms responsible for maintaining integrity and normal function.[6] Several studies of the role of the MEK-ERK pathway on intestinal epithelial differentiation found that this signaling cascade is an important mediator of these processes.[7–9] Recent reports have shown that the activation of ERK protects certain cells from undergoing programmed cell death in response to a variety of agents and that the MEK-ERK pathway modulates the expression and activity of some members of the Bcl family.[10–14] Enterocyte-like terminal differentiation is closely related to eventual programmed cell death.[6] Therefore, the MEK-ERK signaling cascade may also modulate programmed cell death, and alterations in this pathway could affect the tumorigenic potential of intestinal epithelial cells.

Currently, the exact role of the MEK-ERK signaling cascade in colorectal carcinogenesis is still under investigation. Several reports have provided evidence for the

Abbreviations used in this paper: CA-MEK, constitutively activated mitogen-activated protein kinase/extracellular signal–regulated protein kinase kinase; cCAMEK, cytomegalovirus promoter-driven constitutively activated mitogen-activated protein kinase/extracellular signal–regulated protein kinase kinase; CMV, cytomegalovirus; COX-2, cyclooxygenase-2; DMEM, Dulbecco's minimal essential medium; DOX, doxycycline; ERK, extracellular signal–regulated protein kinase; JNK, c-Jun-N-terminal kinase; MAPK, mitogen-activated protein kinase; MEK, mitogen-activated protein kinase/extracellular signal–regulated protein kinase kinase; NaB, sodium butyrate; Tet, tetracycline; tiCAMEK, tetracycline-regulated constitutively activated mitogen-activated protein kinase/extracellular signal–regulated protein kinase kinase.

© 2005 by the American Gastroenterological Association
0016-5085/05/$30.00
doi:10.1053/j.gastro.2005.06.003

activation of these kinases in colorectal cancer. Oncogenic mutations in *ras* are known to result in the activation of downstream signaling proteins, including the Raf-MEK-ERK pathway.[2,5] Mutations in Ras are found in a wide variety of human malignancies, including colorectal cancer.[15] Similar to activated oncogenic *ras*, B-Raf, which is one upstream activator of MEK, has been shown to possess somatic mutations and elevated kinase activities in malignant melanoma, colorectal cancer, and brain tumors.[16] Consistent with those reports, colorectal cancers have particularly high frequencies of ERK activation,[17] and a subset of human colorectal tumors showed elevated levels of ERK relative to normal adjacent colon mucosa.[18,19] Recently, MEK has been shown to be phosphorylated in 76% of colorectal tumors and 30%–40% of adenomas.[20] Conversely, several reports showed no relationship between colorectal cancer and this kinase pathway.[21,22] In addition, the precise outcome of constitutive activation of MEK on intestinal epithelial cell transformation is also unclear. Activation of Raf-1, which is the upstream signal of MEK-ERK, did not transform RIE-1 rat intestinal epithelial cells.[23] On the other hand, a recent study has shown that the overexpression of constitutively active MEK (CA-MEK) in IEC-6 rat intestinal epithelial cells promoted growth in soft agar.[24] Therefore, the involvement of the MEK-ERK pathway in colorectal carcinogenesis remains poorly defined.

The MEK-ERK cascade has been reported to possess some oncogenic potential, including increased tumor invasiveness,[25,26] pro–cell cycle properties,[27] angiogenesis,[28] and resistance to some anticancer agents.[29,30] Therefore, MEK-ERK signaling may play an important role in the development of colorectal cancer and may represent one of the important targets for developing a new therapy for treatment and/or prevention of colorectal cancer. Furthermore, the growth and invasiveness of colon carcinoma xenografted tumors in vivo was dramatically retarded by pharmacologic inhibition of MEK.[31]

Other than the oncogenic potential described previously, MEK signaling has also been associated with cyclooxygenase-2 (COX-2). A growing body of evidence suggests that COX-2 activity and prostaglandin (PG) synthesis may be involved in intestinal carcinogenesis.[32,33] In normal rat intestinal epithelial cells, forced expression of COX-2 provides the cells with a survival advantage.[34] COX-2 is believed to be a target of oncogenic mutated *ras* in a variety of biologic systems.[35–38] Activation of MEK is in part responsible for Ras-mediated induction of COX-2 in intestinal epithelial cells.[35,38] However, the precise role of MEK-ERK signaling on induction of COX-2 in intestinal epithelial cells has not been established.

We sought to determine the oncogenic potential of CA-MEK in RIE-1 cells. RIE-1 cells are nontransformed rat intestinal epithelial cells derived from the normal undifferentiated intestinal crypt.[39] In particular, we evaluated the role of COX-2 and PGs on the antiapoptotic and pro–cell cycle effects of CA-MEK. Here, we show that constitutive activation of MEK signaling contributed to the transformation of rat intestinal epithelial cells via a COX-2–dependent, antiapoptotic mechanism.

Materials and Methods

Cells and Culture Conditions

RIE-1 cells were a gift from Dr K.D. Brown (Cambridge Research Station, Babraham, Cambridge, England). Cells were grown in Dulbecco's minimal essential medium (DMEM) supplemented with 10% heat-inactivated fetal bovine serum (Hyclone Laboratories, Logan, UT) and 2 mmol/L L-glutamine. IEC-6 cells were purchased from American Type Culture Collection (Manassas, VA) and were maintained in DMEM with 10% heat-inactivated fetal bovine serum, 2 mmol/L L-glutamine, and 0.1 U/mL bovine insulin (Sigma Chemical Co, St Louis, MO).

Stable Transfection

Two different types of CA-MEK plasmids were used. The first construct is a tetracycline (Tet)-regulated CA-MEK (tiCAMEK), which induces the expression of CA-MEK in the absence of Tet (doxycycline [DOX]) (Tet-Off). The second construct is a cytomegalovirus (CMV) promoter-driven CA-MEK (cCAMEK).

The RIE-tiCAMEK cell lines with an inducible MEK1 phosphorylation site mutant (a constitutively activated form) complementary DNA were generated by using the Tet-Off gene expression system (BD Biosciences, Palo Alto, CA). The *Xba*I-*Bam*HI (fill-in) fragment containing mouse MEK1 phosphorylation site mutant from pVL1392-MEK1-Glu · Glu[40] (a gift from Dr Alessandro Alessandrini, Massachusetts General Hospital, Charlestown, MA) was subcloned into the *Nhe*I-*Eco*RV site of pBI-L, Tet response vector, and then confirmed by DNA sequencing. RIE-1 cells were transfected with the pTet-off and pBI-L-CA-MEK sequentially. The first transfection was performed with FuGENE 6 transfection reagent (Roche, Indianapolis, IN), and the second transfection was performed using a Cell Phect transfection kit (Amersham Pharmacia, Piscataway, NJ) according to the manufacturer's protocol. Clones were selected and maintained in DMEM containing heat-inactivated 10% Tet system-approved fetal bovine serum (BD Biosciences), 2 mmol/L L-glutamine, 400 μg/mL G418 (Mediatech Inc, Herndon, VA), and 200 U/mL Hygromycin B (Calbiochem, San Diego, CA). DOX (BD Biosciences) at a concentration of 2 μg/mL was used to repress the expression of activated MEK.

The RIE-cCAMEK cells and IEC-cCAMEK cells contained the constitutively expressed MEK1 phosphorylation site mutant complementary DNA under the control of CMV promoter, and the RIE-Mock cells and IEC-Mock cells contained an empty vector (pcDNA3.1Zeo; Invitrogen, Carlsbad, CA). The *Xba*I-*Bam*HI fragment from pVL1392-MEK1-Glu · Glu was subcloned into the *Xba*I-*Bam*HI site of pcDNA3.1Zeo and confirmed by sequence analysis (pCMV-CA-MEK). RIE-1 cells and IEC-6 cells were transfected with pcDNA3.1Zeo or pCMV-CA-MEK using a Cell Phect transfection kit, and clones were selected by growth in culture media containing 100 μg/mL of Zeocin (Invitrogen).

To confirm the involvement of ERK activation by CA-MEK, we also generated sequential transfection of ERK1 or ERK2 dominant negative constructs in RIE-tiCAMEK cells. The ERK1 or ERK2 dominant negative expression vectors, pCEP4-ERK1-DN or pCEP4-ERK2-DN, were gifts from Dr Melanie Cobb (University of Texas, Southwestern, TX). To establish RIE-tiCAMEK/ERK1-DN cells, or RIE-tiCAMEK/ERK2-DN cells, or RIE-tiCAMEK/Mock cells, RIE-tiCAMEK cells were cotransfected with pCEP4-ERK1-DN, or pCEP4-ERK2-DN, or pCEP4 plasmid and pcDNA3.1Zeo plasmid, respectively. Cells were selected by growth in media containing 150 μg/mL of Zeocin, and isolated clones were used for the study.

Soft Agarose Assay

Soft agarose assays were performed as previously described.[41] Briefly, 1×10^4 cells were mixed with Sea plaque agarose (BioWhittaker, Walkersville, MD) at a final concentration of 0.4% in DMEM and overlaid onto a 0.8% agarose layer in 35-mm plates. The plates were incubated for 10–16 days, following which colonies were photographed and counted. Colony number was manually counted and is expressed as the number of colonies per plate.

Tumor Xenografts in Nude Mice and Terminal Deoxynucleotidyl Transferase-Mediated Deoxyuridine Triphosphate Nick-End Labeling Staining

A total of 5×10^6 cells suspended in 0.1 mL DMEM were injected into the dorsal subcutaneous tissue of nude mice (Sprague–Dawley nu/nu; Harlan, Indianapolis, IN). Tumor volume was determined by external measurement according to published methods[42] and using the equation $V = (L \times W^2) \times 0.5$, where V is volume, L is length, and W is width.

For the COX-2 inhibitor treatment study, 1×10^6 cells suspended in 0.2 mL DMEM were injected into the dorsal subcutaneous tissue of athymic nude mice. A COX-2–selective inhibitor (celecoxib; a kind gift from G.D. Searle and Co, St. Louis, MO) was suspended in 0.5% (wt/vol) methylcellulose and 0.1% (vol/vol) polysorbate 80 and dissolved in water by constant stirring. Mice were given celecoxib (100 mg/kg) or vehicle daily by gavage tube. Doses of celecoxib >100 mg/kg are expected to produce some COX-1 inhibition, whereas lower doses would selectively inhibit COX-2.[43] The treatment was continued for 17 days, and then tumors were removed from the mice and fixed in 10% formalin for 24 hours. Fragmented DNA indicating apoptotic cells was visualized with the DeadEnd Colorimetric TUNEL System (Promega, Madison, WI). After fixation, tissues were embedded into paraffin blocks. Five-micrometer tissue sections were placed on charged slides, deparaffinized, and rehydrated. The tissue sections were subjected to a second fixation in 4% paraformaldehyde, rinsed, and permeabilized with proteinase K for 5 minutes. The sections then were treated with equilibration buffer (Promega) followed by biotinylated nucleotide incorporation into apoptotic cells using terminal deoxynucleotidyl transferase. Endogenous peroxidase was neutralized by applying 0.3% hydrogen peroxide to the sections. Applications of streptavidin/horseradish peroxidase and 3,3′-diaminobenzidine tetrahydrochloride produced apoptotic-specific visible nuclear staining. The slides were lightly counterstained with Mayer's hematoxylin, dehydrated, and coverslipped. The numbers of apoptotic cells were quantified with a Nikon Eclipse 80i microscope (Boyce Scientific, Gray Summit, MO) using analysis-OPTI imaging analysis software (Soft Imaging Systems, Lakewood, CO).

Cell Viability and Apoptosis Assay

RIE-tiCAMEK cells treated with 2 μg/mL DOX or vehicle, RIE-cCAMEK cells, and RIE-Mock cells were seeded into 60-mm plates. After 48 hours, the culture media was replaced with media containing 5 mmol/L sodium butyrate (NaB; Sigma Chemical Co) (for RIE-tiCAMEK cells also containing 2 μg/mL DOX or vehicle, a half dose of DOX was added after 72 hours). Before starting treatment with NaB, cells had reached 85%–90% confluency. After 4 days, the cells were harvested and stained with Annexin V/fluorescein isothiocyanate and/or propidium iodide using a TACS Annexin V/Fluorescein Isothiocyanate Apoptosis Detection Kit (R&D Systems, Minneapolis, MN). The samples were analyzed by flow cytometry, and cell numbers were also determined manually using a hemacytometer. Viable cells were distinguished using the trypan blue dye exclusion method.[44]

Immunoblot Analysis and Antibodies

Cells were lysed with cell lysis buffer (50 mmol/L HEPES, pH 7.5, 150 mmol/L NaCl, 1 mmol/L EDTA, 0.1% Triton X-100, 1 mmol/L phenylmethylsulfonyl fluoride, 0.5 mmol/L sodium orthovanadate, 10 mmol/L β-glycerophosphate, and 4 μg/mL each of leupeptin and antipain) at 4°C for 10 minutes. The cell lysate (5–100 μg/lane) was denatured and fractionated by sodium dodecyl sulfate/polyacrylamide gel electrophoresis. After electrophoresis, the proteins were transferred to polyvinylidene difluoride transfer membrane (PolyScreen; NEN Life Science, Boston, MA) and the filters then probed with the indicated antibodies and developed by enhanced chemiluminescence (Amersham, Piscataway, NJ). The anti-GluGlu (EE) antibody was purchased from Covance (Richmond, CA). The anti–phospho-ERK (Thr^{202}/Tyr^{204}),

anti-ERK, anti–phospho-Akt (Ser^{473}), anti-Akt, anti–phospho-p38 (Thr^{180}/Tyr^{182}), anti-p38, anti–Bcl-X, and anti–cyclin D1 antibodies were purchased from Cell Signaling Technology (Beverly, MA). The anti–Bcl-2 and anti-$p21^{Cip/WAF1}$ antibodies were purchased from Oncogene Research Products (Boston, MA). The anti-Bax, anti-Bak, and anti-Bad antibodies were purchased from BD Biosciences. The anti–COX-2, anti–Bag-1, anti–Mcl-1, anti–cdk4, anti-cdk2, anti–cyclin E, anti-p15, and anti-$p27^{Kip}$ antibodies were purchased from Santa Cruz Biotechnology (Santa Cruz, CA). The anti–β-actin antibody was purchased from Sigma Chemical Co.

In Vitro Phosphorylation of Bad-Agarose Substrate Assay

To determine the in vitro phosphorylation of recombinant Bad protein, the Bad ($Ser^{112/136}$) Phosphorylation Detection Kit (Upstate Biotechnology, Lake Placid, NY) was used. Briefly, cells of each group were established in 60-mm^2 plates and cultured in media containing 5 mmol/L NaB for an additional 72 hours. The assay was performed according to the manufacturer's protocol.

Flow Cytometry

RIE-tiCAMEK cells were seeded into 100-mm plates and treated with 2 μg/mL DOX or vehicle (dH_2O) for 48 hours. The medium was then replaced with 2 μg/mL DOX or vehicle plus 5 mmol/L NaB. After 72 hours, the DNA was analyzed by flow cytometry, and the cell cycle profile was expressed as percentage of cells in each cell cycle stage.

Quantitation of Eicosanoids

For RIE-tiCAMEK cells, after pretreatment with DOX or vehicle for 48 hours, subconfluent cells were established; the cells were then treated with 5 mmol/L NaB plus 2 μg/mL DOX or vehicle for an additional 48 hours. Serum-free DMEM with 10 μmol/L arachidonic acid (Cayman, Ann Arbor, MI) was replaced 1 hour before collecting the conditioned medium. Levels of 6-keto $PGF_{1\alpha}$ and PGE_2 were quantified by using a gas chromatography/negative ion chemical ionization mass spectrometric assay as described.[45] RIE-cCAMEK and RIE-Mock cells were also subjected to the assay as described previously. The results are expressed as nanograms of 6-keto $PGF_{1\alpha}$ or PGE_2 per 10^5 cells.

Transfection of COX Reporter Constructs

The assays to determine the activity of the *COX-2* promoter were performed as previously described.[46] Reporter constructs phPES2 (−1432/+59, −327/+59, −220/+59, −124/+59, −52/+59, CRM, ILM, and CRM-ILM) containing the 5′-flanking region of the human *COX-2* gene were described previously.[46] For transient transfections, cells were plated in 24-well plates 24 hours before transfection and cotransfected with 0.5 μg of one of the COX-2 firefly luciferase plasmid constructs and 0.02 μg of the pRL-TK plasmid, containing the *Renilla* luciferase gene (Promega), using FuGENE 6 transfection reagent. Fourteen hours after transfection, media containing 5 mmol/L NaB was replaced; the cells were cultured for an additional 24 hours and then harvested. Twenty microliters of cell lysate was used for both the firefly and the *Renilla* luciferase readings. Firefly and *Renilla* luciferase activities were measured using a dual-luciferase reporter assay system (Promega) in a model TD-20/20 luminometer. Firefly luciferase values were standardized to *Renilla* values as previously reported.[46]

Northern Blot Analysis

For the determination of COX-2 messenger RNA (mRNA) expression levels, RIE-tiCAMEK cells with DOX or vehicle were treated with 5 mmol/L NaB for 48 hours. RNA samples were isolated using TRIzol reagent (Invitrogen) according to the manufacturer's protocol. For determination of mRNA stability, cells were treated with 5 mmol/L NaB for 24 hours and then the transcription was stopped by the addition of 100 μmol/L of 5,6-dichlorobenzimidazole riboside (Sigma Chemical Co). RNA samples were isolated at 0, 15, 30, 45, and 60 minutes following treatment with 5,6-dichlorobenzimidazole riboside and analyzed for COX-2 levels by Northern blot analysis. Northern blot analysis was performed as described previously.[47]

Statistical Analysis

Data were analyzed by Student *t* test using the StatView software program (SAS Institute, Inc, Cary, NC). Data were considered significant if $P < .05$, and individual *P* values are indicated in the figure legends.

Results

MEK Activation Induces the Transformation of Cultured Intestinal Epithelial Cells

To address the role of the MEK-ERK signaling pathway in the transformation of intestinal epithelial cells, we generated RIE-1 and IEC-6 cells that stably express CA-MEK. MEK1 is activated by phosphorylation at Ser^{218} and Ser^{222} by members of the Raf family of kinases.[48] Mutation of these 2 sites to acidic residues, specifically Asp^{218} and Asp^{218}/Asp^{222}, results in CA-MEK1.[49] The Asp^{218}/Asp^{222} MEK1 phosphorylation site mutant has previously been shown to activate ERK1/2 and to transform NIH3T3 fibroblasts.[49]

One important characteristic of transformed cells in vitro is their ability to grow in an anchorage-independent manner in soft agarose. Therefore, cells expressing CA-MEK were tested for their ability to form colonies in soft agarose. In agreement with a recent report,[24] CA-MEK–expressing rat intestinal epithelial cells, both RIE-1 (RIE-cCAMEK, clones DD13 and

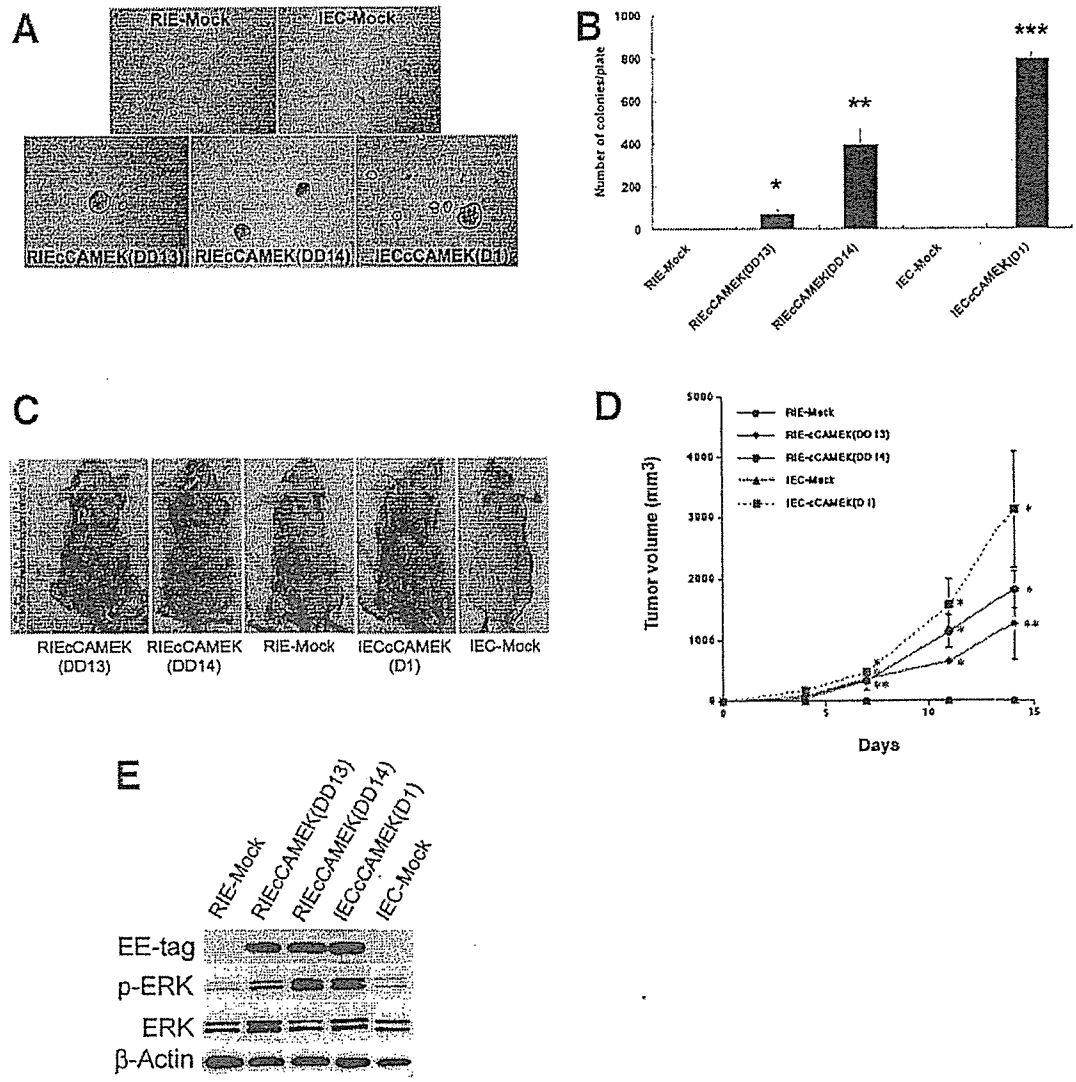

Figure 1. Transformation of rat normal intestinal epithelial cells by CA-MEK. (*A* and *B*) Anchorage-independent growth of cCAMEK stable transfected RIE-1 cells (clone DD13, DD14) and IEC-6 cells (clone D1) in soft agarose. The plates were incubated for 13 days, following which colonies were photographed and counted from triplicate plates of cells. Colony number was manually counted and is expressed as the number of colonies per plate. Values are the means ± SE of 3 separate experiments performed in triplicate. $*P = .0027$, $**P = .0008$, $***P < .0001$ compared with mock cells. (*C* and *D*) Athymic nude mice subcutaneously injected with either CA-MEK transfected cells (RIE-DD13, RIE-DD14, IEC-D1) or empty vector (pcDNA3.1) transfected cells (Mock) were evaluated. n = 3 mice per group. Values are the means ± SD of each of 3 independent xenografts. $*P < .01$, $**P < .05$ compared with mock control. (*E*) Western blot analysis of EE-tagged CA-MEK, phospho-ERK1/2, ERK1/2, and β-actin protein levels in cultured cells described previously.

DD14) and IEC-6 cells (IEC-cCAMEK, clone D1 and D2), formed colonies in soft agarose, whereas empty vector transfected cells (RIE-Mock and IEC-Mock) did not (Figure 1*A* and *B*; data not shown).

To test for tumor formation in vivo, CA-MEK–expressing cells were injected subcutaneously into nude mice. Whereas RIE-Mock and IEC-Mock cells did not form tumors, all CA-MEK transfected RIE and IEC cell lines formed rapidly growing tumors (Figure 1*C* and *D*). Histologic examination showed that the tumors that formed in vivo were undifferentiated adenocarcinomas that were highly invasive with neovascularization (data not shown). Western blot analysis identified elevated levels of EE-tagged MEK1 and phosphorylated ERK1/2 expression in CA-MEK–expressing cells (Figure 1*E*). Because we generated these cells by stably expressing an epitope-tagged CA-MEK, elevated levels of EE signal represented the level of cellular transgene expression. Thus, this result shows that the MEK-ERK signaling pathway contributes to neoplastic transformation of rat intestinal epithelial cells.